PHOTOPROTONS FROM Cu^{65}

N. V. LIN'KOVA, R. M. OSOKINA, B. S. RATNER, R. Sh. AMIROV* and V. V. AKINDINOV*

P. N. Lebedev Physical Institute, Academy of Sciences, U.S.S.R.

Submitted to JETP editor October 5, 1959

J. Exptl. Theoret. Phys. (U.S.S.R.) **38**, 780-789 (March, 1960)

The energy and angular distributions of photoprotons produced in a Cu^{65}-enriched sample by bremsstrahlung with maximum energies $E_{\gamma max}$ = 17.9, ~ 20, 24.5, and 28.5 Mev were studied by means of photographic emulsions. The dependence of the Cu^{65} photoproton yield on $E_{\gamma max}$ was measured and the excitation curve for reactions involving proton emission was determined. An analysis of the experimental data shows that at least 80% of the proton yield is due to a mechanism other than evaporation. If this mechanism is assumed to be a direct photoeffect in which all the gamma-ray energy minus the binding energy is imparted to the ejected proton it is found from the energy distributions that only a small fraction of the protons results from the photoeffect at the highest nuclear level, the principal contribution being due to transitions from lower-lying shells. Two proton emission peaks are observed, E_p = ~ 4.7 and ~ 6.0 Mev. The angular distributions are represented by $a + b \sin^2 \theta$ for $E_{\gamma max}$ = 17.9 and 20.0 Mev, and by $a + b \sin^2 \theta + c \sin^2 \theta \cdot \cos^2 \theta$ for $E_{\gamma max}$ = 24.5 and 28.5 Mev. This indicates dipole absorption of gamma rays for E_γ < 20 Mev, with quadrupole absorption becoming appreciable at higher energies.

INTRODUCTION

IN investigating the mechanism of interactions between gamma rays and nuclei valuable information is obtained by studying angular and energy distributions and the yields of photonuclear products. The observed departures from statistical theory for the (γp) reaction[1-3] have suggested the existence of a direct nuclear photoeffect,[4] although details of this mechanism and the part it plays in giant resonance have thus far not been determined. It is of special interest to investigate the (γp) reaction in isotopes where proton evaporation is not favored. The direct photoeffect is an important participant in the (γp) reaction for $Z \approx 28$.[5,6] For example, in a natural mixture of copper isotopes it accounts for $20 - 40\%$ rather than $5 - 10\%$ as previously estimated.[3,7] We used a Cu^{65}-enriched sample for the purpose of verifying these results.

According to statistical theory, if all other conditions are identical proton evaporation is limited by competition with neutron evaporation and is strongly dependent on the difference between the neutron binding energy B_n and the proton binding energy B_p. The ratio of proton to neutron emission probability w_p/w_n contains the factor $\exp \{ B_n - B_p \}$.[8] On the basis of the binding energy ratio in Cu^{63} and Cu^{65} the proton evaporation yield from Cu^{65} should be only about one-tenth as large as from Cu^{63}.

We may therefore expect that the contribution of the direct photoeffect to the (γp) yield from copper should increase with the Cu^{65} content. Preliminary data[9] have shown that the ratio of (γp) yields in Cu^{65}-enriched and natural copper samples for $E_{\gamma max}$ = 29.0 Mev is considerably greater than that predicted by the statistical theory. An estimate of ~ 85% for the direct photoeffect in Cu^{65} and ~ 40% in Cu^{63} was confirmed by an analysis of angular and energy distributions of photoprotons from natural copper.[5] A subsequent more careful measurement of the photoproton energy distribution from Cu^{65} for $E_{\gamma max}$ = 19.5, 24.5, and 28.5 Mev revealed separate peaks in the spectrum,[10] although the statistical accuracy was unsatisfactory and additional measurements were performed to provide the necessary confirmation. All data for Cu^{65} are summarized in the present paper.

EXPERIMENTAL PROCEDURE

Nuclear emulsions were used in this work. Figure 1 shows the experimental arrangement including the interior geometry of the chamber containing the target and plates. The target was a 29 mg/cm^2 foil containing 93.5% Cu^{65} and 6.5% Cu^{63}. The plates were positioned on both sides of the target at angles θ equal to 30, 50, 70, 90, 110, 130, and 150° with respect to the gamma-ray direction (Fig. 1a), except in the case of $E_{\gamma max}$

---

*At Saratov State University.

FIG. 1. Experimental arrangement: A — lead colli-
mator, B — lead shield, C — sweeping magnet, D — vac-
uum chamber containing target and plates, E — monitor,
F — paraffin, G — lead. a — interior geometry of chamber;
dashed lines represent plate positions for yield mea-
surements; b — the same for irradiation at $E_{\gamma max} = 20.0$
Mev; 1 — target, 2 — plates.
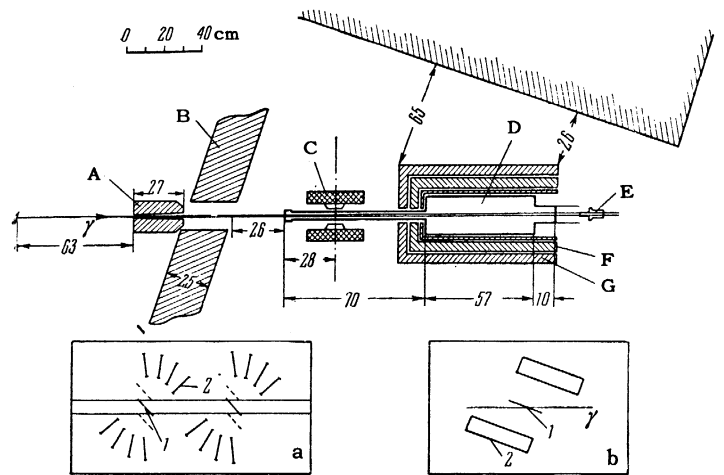
= 20.0 Mev, the geometry for which is shown in
Fig. 1b. Plates located close to the target were
also irradiated in order to determine the yield
curve at low energies ($E_{\gamma max} < 18$ Mev) and to
determine the photoproton yield ratio from Cu^{65} -
enriched and natural copper samples.

Protons were registered in NIKFI Ya-2 and
T-3 emulsions of 300μ and 400μ thicknesses.
Dosages were monitored by an integrating ioni-
zation chamber which was calibrated by a thick-
walled ionization chamber of known sensitivity.

The results given below were corrected only
for the scattered gamma-ray background, which
was measured in the absence of the target. This
background was small (1 — 5%) and was concen-

trated mainly in the low proton-energy region ϵ_p
< 5 — 7 Mev.

An additional background associated with the
target cannot easily be evaluated quantitatively.
We shall now proceed to estimate the contribu-
tions of the principal processes.

1. (γd) and ($\gamma \alpha$) reactions. The emulsions
used in the present work do not permit very good
discrimination of charged-particle tracks. There-
fore we assigned to the effect in question all tracks
starting at the emulsion surface, moving in the
required direction and having lengths correspond-
ing to proton energies $\epsilon_p \geq 3$ Mev. We thus ac-
tually measured the results of the combined reac-
tions (γp) + (γnp) + (γd) + ($\gamma \alpha$).

FIG. 2. Energy distributions of photoprotons
from Cu^{65} for different values of $E_{\gamma max}$. Statis-
tical errors are indicated.
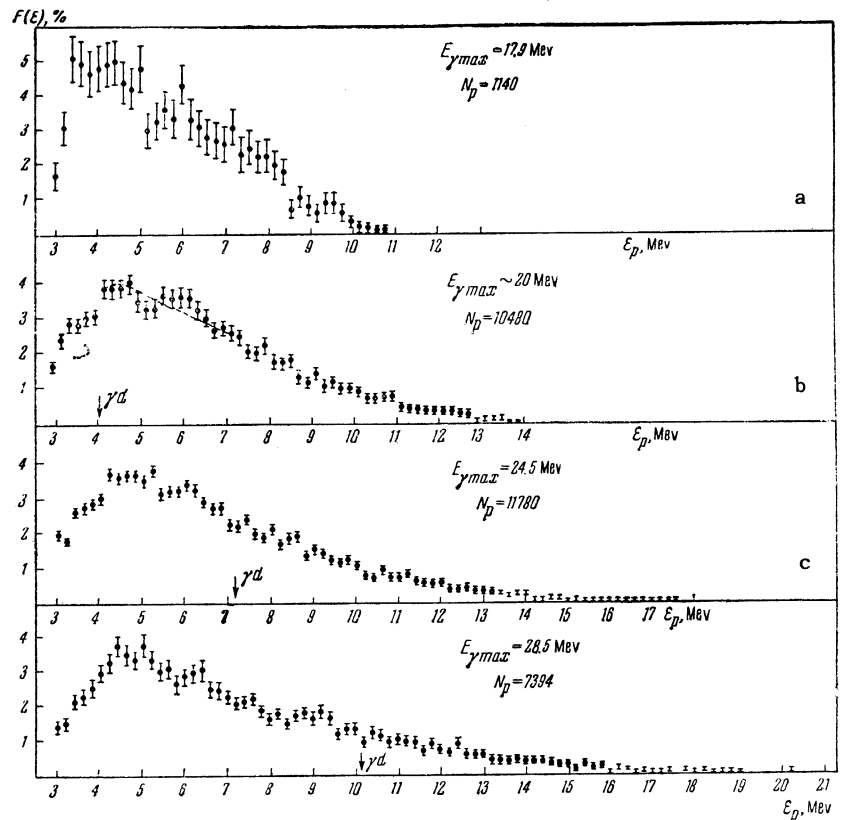
Rough estimates of the contributions of the (γd) and ($\gamma\alpha$) reactions, based on measurements obtained from natural copper,[3,11,12] indicate that the photodeuteron contribution is not greater than 10% (for $E_{\gamma max}$ > 25 Mev) while the contribution of alpha particles may be disregarded altogether. For lower values of $E_{\gamma max}$ this contribution will obviously be still smaller.

2. Contribution from Cu^{63}. The sample contained about 6.5% Cu^{63}. An estimate based on the measured photoproton yield ratio of natural and Cu^{65}-enriched samples indicates that Cu^{63} contributed 10 − 15% for all four values of $E_{\gamma max}$.

EXPERIMENTAL RESULTS

The proton energy spectra in Fig. 2, for $E_{\gamma max}$ = 17.9, ~ 20, 24.5, and 28.5 Mev, represent combined measurements obtained with plates that were placed at different angles θ with respect to the gamma-ray beam. The total numbers N_p of tracks used in plotting the spectra were 1140, 10,480, 11,780, and 7394, respectively, for the different values of $E_{\gamma max}$. Relative units are used. F (ϵ) is the ratio of the number of tracks in the $\epsilon_p \pm 0.1$ Mev interval to the number with $\epsilon_p \geq 3.0$ Mev. Arrows indicate the proton energy limit below which the spectra may be distorted by photodeuterons.

The spectra were plotted with special care in order to determine whether a structure is present. We first plotted for each plate a histogram of the track number N (L) in the length interval ΔL = 5 μ as a function of measured track length L. A correction for proton energy loss in the target was then introduced by shifting the range scale toward larger values by an amount l equivalent in a given plate to half of the target thickness. (The average energy loss was 0.5 Mev for ϵ_p = 5 Mev and ~ 0.3 Mev for ϵ_p = 11 Mev.) Using the ranges L′ = L + l and the corresponding energies with 0.2-Mev intervals in accordance with the range-energy curve we computed the number of tracks in each energy interval and subtracted the background. The range-energy curve for Ilford C-2 emulsions[13] was used for the NIKFI Ya-2 emulsion. The NIKFI T-3 emulsion, which contains a little less AgBr than the Ilford C-2, was calibrated according to the recoil-proton range produced by 14-Mev neutrons and the aforementioned range-energy curve was corrected. Range intervals $\Delta L'$ corresponding to energy intervals $\epsilon_p \pm 0$. Mev were determined very carefully, with special attention to the monotonic increase of these intervals with ϵ_p. The proton
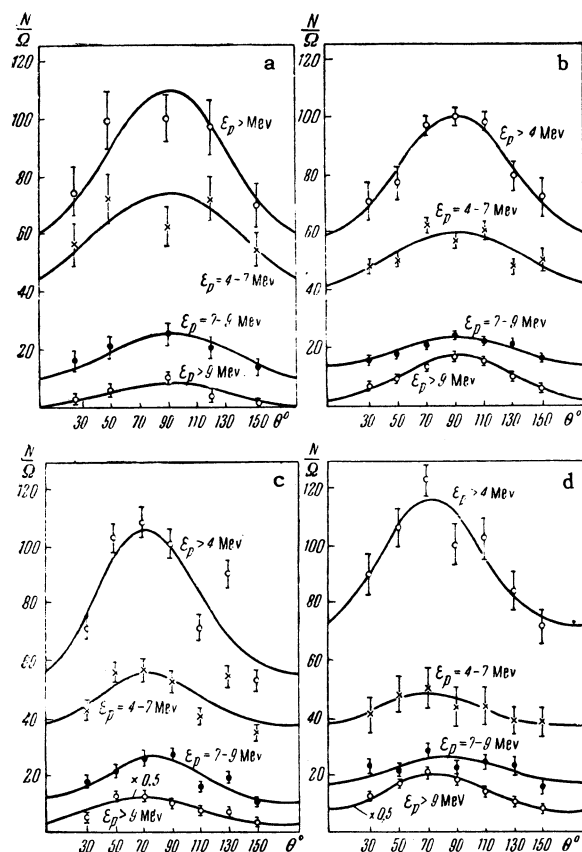

FIG. 3. Angular distributions of photoprotons from Cu^{65} (in relative units): (a) $E_{\gamma max}$ = 17.9 Mev, (b) 20.3 Mev, (c) 24.5 Mev, (d) 28.5 Mev. The number of protons with energies $\epsilon_p \geqslant 4$ Mev is taken as 100. Statistical errors are indicated.

spectra were thus free of possible peaks resulting from systematic errors associated with inaccurate determination of the intervals $\Delta L'$.

Figure 3 shows the angular distributions of photoprotons for the different energy groups. The continuous curves represent the following distributions:

$$I (\theta) = a + b \sin^2 \theta \quad \text{(Fig. 3a and b)} \quad (1)$$

$$I (\theta) = a + b \sin^2 \theta + c \sin^2 \theta \cos \theta \, \text{(Fig. 3c and d)} \quad (2)$$

The following table contains the least-squares values of b/a and c/b.

In Fig. 4 the photoproton yield of a Cu^{65}-enriched sample is shown as a function of $E_{\gamma max}$; data obtained at different times are connected by the curves. The yield is given for unit solid angle and identical ionization in a thick-walled ionization chamber. The curve may be attributed primarily to (γp) and (γnp) reactions in Cu^{65}, the cross section for which (denoted by $\sigma_{\gamma p}$ for brevity) is shown in Fig. 5. The cross sections were calculated from the yield curve by the method of photon differences.[14] The absolute normalization of this curve will be discussed below.

Parameters in the Angular Distribution of Protons.

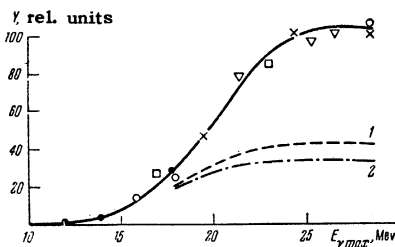| ϵ_p, Mev	$E_{\gamma\,max} = 17.9$ Mev	20.0 Mev	24.5 Mev		28.5 Mev	
	b/a	b/a	b/a	c/b	b/a	c/b
≥4	0.81	0.68	0.76	0.79	0.52	0.86
4—7	0.50	0.87	0.40	0.83	0.22	0.19
7—9	1.60	0.75	1.20	0.69	0.47	0.42
>9	83	10.0	1.90	0.87	1.23	0.91

FIG. 4. Cu^{65} photo-proton yield as a function of E$_{\gamma\,max}$. Different symbols represent different sets of data. The broken lines were calculated from the statistical model: curve 1 for a = 16 Mev^{-1};[15] curve 2 for a = 8 Mev^{-1}.[16]
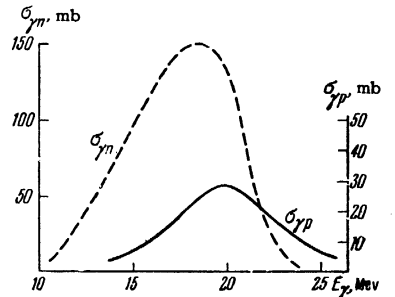

FIG. 5. Cross section for Cu^{65} photoproton emission. The dashed curve provides comparison with the cross section for Cu^{65}(γn)Cu^{64}.[17]

DISCUSSION OF RESULTS

1. Photoproton yield from Cu^{65}. Using the measured photoproton yield ratio for natural copper and a Cu^{65}-enriched sample (1.5 ± 0.2 for Eγmax = 25.2 Mev) and the fractional isotopic abundance of Cu^{63} and Cu^{65} in the samples, the photoproton yield ratio from these isotopes at the given Eγmax was found to be 1.9. By comparison, the statistical theory of nuclear reactions gives the value 9 for the ratio. The calculation resembled that of Byerly and Stephens,[3] assuming $\omega(E_R) \sim \exp(aE_R)^{1/2}$ for the level density in both final nuclei Ni^{62} and Ni^{64}. The following constants were used: $a_1 = 3.35(A-40)^{1/2} \approx 16$ Mev^{-1},[15] $a_2 = 8$ Mev^{-1};[16] $r_0 = 1.5 \times 10^{-13}$ cm; $\sigma_{\gamma n}$ was taken from reference 17. The proton binding energy B$_p$ and the neutron binding energy B$_n$ were taken to be 6.5 and 11.0 Mev, respectively, in Cu^{63} and 7.5 and 10.0 Mev in Cu^{65}.

It should be noted that the assumption of equal level densities in Ni^{62} and Ni^{64} is not strictly justified. There are indications of considerable fluctuations of nuclear-level density near magic numbers.[18,19] If it should be found that the level density in Ni^{64} is 4 or 5 times greater than in Ni^{62} the observed proton yield ratio for Cu^{65} and Cu^{63} would not disagree with statistical theory. However, Ni^{64} and Ni^{62} differ only[20] by the circumstance that in the unfilled 4f$_{5/2}$ neutron level the former contains two neutrons while the latter contains two vacancies; we can therefore hardly expect the level densities to differ so strongly. The statistical theory also cannot account for the sharp rise of the photoproton yield in the region Eγmax = 20 — 25 Mev (Fig. 4). To account for these facts it must be assumed that most of the Cu^{65} proton yield results from a mechanism other than evaporation. A calculation based on the assumption that the proton yields from Cu^{65} and Cu^{63} as a result of evaporation differ by a factor of 9 indicates that this additional mechanism contributes at least 80% to the Cu^{65} photoproton yield.

2. Energy distributions. The photoproton spectra in Fig. 2 are marked by the following characteristics:

a) Although a large fraction of the proton yield is apparently produced by a mechanism different from evaporation (at least for Eγmax = 24.5 and 28.5 Mev) a considerable fraction of the protons is found at relatively low energies (ϵ_p = 4 — 6 Mev).

b) The fraction of protons close to the maximum possible energy, $\epsilon_p$max = Eγmax − B$_p$, is small and falls off sharply as Eγmax increases. It therefore is a relatively infrequent occurrence that the entire energy of a gamma ray, minus the binding energy, is transferred to a proton from an upper level. This conclusion follows even more convincingly from an examination of proton spectra produced by gamma rays in narrower energy intervals. In work on bremsstrahlung such spectra can be obtained by taking the differences between proton spectra measured at two values of Eγmax and normalized to unit solid angle and identical ionization in a thick-walled ionization chamber. Figure 6 shows such differences between proton spectra,

$$\Delta Y(\epsilon) = [YF(\epsilon)]_{E_{\gamma max}^{(1)}} - [YF(\epsilon)]_{E_{\gamma max}^{(2)}};$$

Y and F(ϵ) are taken from Figs. 2 and 4, respectively. The corresponding bremsstrahlung spectra are also shown:
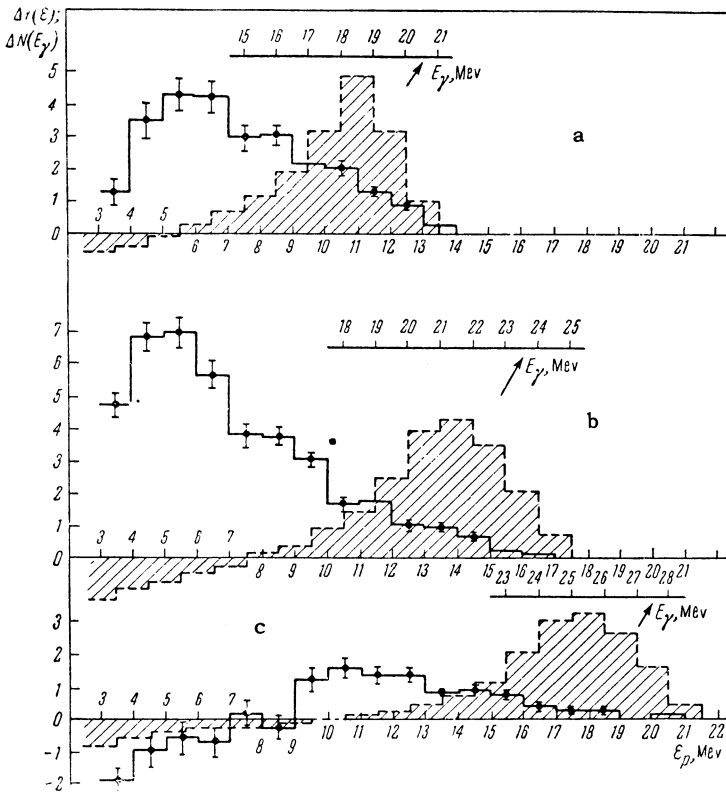
FIG. 6. Differences between proton spectra: a — for $E^{(1)}_{\gamma max}$ = 20.0 Mev and $E^{(2)}_{\gamma max}$ = 17.9 Mev; b — for $E^{(1)}_{\gamma max}$ = 24.5 Mev and $E^{(2)}_{\gamma max}$ = 20.0 Mev; c — for $E^{(1)}_{\gamma max}$ = 28.5 Mev and $E^{(2)}_{\gamma max}$ = 24.5 Mev. The dashed lines represent the differences between the corresponding bremsstrahlung spectra.

$$\Delta N\,(E_\gamma) = N\,(E_\gamma,\; E^{(1)}_{\gamma max}) - N\,(E_\gamma,\; E^{(2)}_{\gamma max}),$$

also reduced to identical ionization. The differences of the proton and gamma-ray spectra are given in arbitrary units, with the gamma-ray energy scale shifted by an amount equal to the proton binding energy B_p = 7.5 Mev. It is consequently evident that protons emitted from the upper level should overlap the gamma-ray spectrum. Figure 6a shows a considerable fraction of these protons overlapping the gamma-rays from 17 to 20 Mev. For E_γ > 20 Mev this fraction is small (Fig. 6b and c).

The proton spectrum in Fig. 6b, corresponding to gamma rays from 19 to 24 Mev, contains a large number of slow protons with ϵ_p from 3 to 8 Mev. Therefore the sharp rise of the yield in this gamma-ray region (Fig. 4) results mainly from the emission of low-energy particles which cannot be attributed to evaporation, since (as already indicated) the statistical theory does not account for the observed rise of the yield; no important change results when the (γnp) process is taken into account. In the case of direct interactions the presence of a large number of slow particles may result either from the large part played by processes in which gamma-ray energies are transferred to two or more particles simultaneously or because there is a large probability for nucleon extraction from deep shells.

The available experimental data do not definitely favor either of these explanations. If we assume that a single-particle mechanism exists, then from the difference ΔE between the proton and gamma-ray peaks in Fig. 6b we can roughly estimate the proton binding energy B_p at the level making the principal contribution to the Cu^{65} photoproton yield. In the case of copper this is most likely the filled $4f_{7/2}$ level. It is easily seen that $B_p\,(4f_{7/2}) \approx \Delta E$ ~ 15 — 16 Mev.

It is of interest that in the spectrum of protons from gamma rays with energies 24 — 28 Mev in Fig. 6b there are no particles with ϵ_p < 9 Mev and that ΔE derived from this figure is also ~ 15 Mev. Gamma rays in the given energy region thus evidently extract protons from the $4f_{7/2}$ level.

c) In the proton spectrum for all four energies two peaks are observed at ϵ_p ~ 4.7 and 6.0 Mev, which are most pronounced for $E_{\gamma max}$ = 20.0 Mev. We attempted to approximate the proton spectrum in the region ϵ_p = 4 — 7 Mev for the given value of $E_{\gamma max}$ by means of the smooth curve represented by the broken line in Fig. 2b. The χ^2 goodness of fit of this curve is defined by

$$Z^2 = \sum_i (F_i\,(z) - \bar{y}_i)^2 / \sigma^2_i,$$

where $F_i\,(\epsilon)$ is the experimental value, $\bar{y}_i$ is the curve ordinate and σ_i is the root-mean-

square error of $F_i(\epsilon)$. The probable validity of the curve was estimated to be about 10%.

Statistical fluctuations can therefore evidently not account for the observed peaks in the proton spectrum. All other errors associated with finite target thickness and experimenters' errors would result in the smoothing of the spectral shape rather than in peaks.

The presence of two peaks in the energy distribution might be attributed to the observation of two spectra with noncoinciding maxima. Possible sources could be, for example, 1) (γp) and (γnp) reactions; 2) photoprotons from Cu^{65} with Cu^{63} admixture; 3) photoprotons resulting from evaporation as well as from a direct photoeffect.

The first of these possibilities cannot account for the presence of two peaks, which are most pronounced for $E_{\gamma\,max} = 20$ Mev, where the (γnp) reaction in copper is possible energetically only with $\epsilon_p < 4$ Mev. When a correction is made for protons from Cu^{63} (from measurements on natural copper[5]) or for the evaporation contribution the observed peaks do not disappear, since in both instances it is necessary to subtract the spectrum with a broad peak in the ϵ_p region from 4 to 6 Mev. The observed peaks therefore do not appear to result from the superposition of two noncoinciding spectra.

Separate peaks in the proton spectrum might also result from transitions between distinct states of the initial and final nuclei, accompanied by proton emission. In our case nuclei are irradiated with continuous bremsstrahlung; therefore distinct initial states can be excited only if the gamma-ray absorption cross section exhibits resonances.

It would be strange if distinct final states were singled out, because of the high nuclear-level density for $A > 50$. It should be noted, however, that proton spectra from the (np) reaction with 14-Mev neutrons and $A > 50$ also sometimes exhibit peaks.[21,22]

3. Angular distributions. Figure 3a shows that the angular distributions of photoprotons for $E_{\gamma\,max} = 17.9$ and 20.3 Mev is quite well approximated by (1). For $E_{\gamma\,max} = 24.5$ and 28.5 Mev (Fig. 3b) the peaks are shifted forward and these distributions are represented by (2).

The table shows that the anisotropy b/a is always appreciably different from zero and that for given $E_{\gamma\,max}$ it increases with ϵ_p. This rise is most pronounced for $E_{\gamma\,max} = 17.9$ and 20.0 Mev, where the angular distribution of the most energetic pronouns, resulting from the photoeffect involving the upper level ($\epsilon_p > 9$ Mev), becomes, as in the case of ordinary copper,[3,5] practically

completely anisotropic: $I(\theta) \sim \sin^2\theta$. According to the models of Courant[4] and Wilkinson[23] such a distribution corresponds to transitions from the S shell and cannot be the result of a photoeffect in the upper $3p_{3/2}$ proton level in copper. However, it was shown in reference 24 that a completely anisotropic distribution may accompany a photoeffect in a P shell if interference of the $l \to l+1$ and $l \to l-1$ transitions is taken into account. It is significant that the angular distribution of fast photoprotons from silver, which also has an upper p level, is likewise represented by $I(\theta) \sim \sin^2\theta$.[25] The diminished fast-proton anisotropy as we go to $E_{\gamma\,max} = 24.5$ and 28.5 Mev is, as in the case of natural copper,[5] apparently associated with the fact that a photoeffect in the lower-lying $4f_{7/2}$ level begins to play a part.

It follows from the 90° peak of the angular distributions for $E_{\gamma\,max} = 17.9$ and 20.0 Mev that for $E_\gamma < 20.0$ Mev gamma-ray absorption is of dipole character. The forward shift of the peak ($c \neq 0$) at higher values of $E_{\gamma\,max}$ indicates that quadrupole absorption is beginning to appear. It can easily be shown that the lower limit of the ratio between the integrated quadrupole and dipole gamma absorption cross sections is given by $\sigma_q^{int}/\sigma_{dip}^{int}$ $(c/b)^2/10\,(3a/b + 2)$, which is estimated to be $\sim 1\%$ for $E_{\gamma\,max} = 24.5$ and 28.5 Mev (for $\epsilon_p > 4$ Mev).

4. Proton emission cross section. The cross section $\sigma_{\gamma p}$ is represented in Fig. 5, with the Cu^{65}(γn)Cu^{64} cross section shown for comparison.[17] $\sigma_{\gamma p}$ has a half-width of about 7 Mev and peak $E_{\gamma p}^{max} = 20.0$ Mev, shifted upward by about 1.5 Mev compared with $\sigma_{\gamma n}$.

By using the known[3,17] ratios of the photoproton and photoneutron yields from Cu^{63} and Cu^{65} together with our own data we determined the absolute maximum of $\sigma_{\gamma p}$ through a comparison with the cross section for Cu^{63}(γn)Cu^{62}.[17] From $\sigma_{\gamma p}^{max}$ (Cu^{65}) = 27 mb obtained in this manner we have $\sigma_{\gamma p}^{int}$(Cu^{65}) = 190 Mev-mb.

It was shown above that at least 80% of the Cu^{65} proton yield results from a mechanism other than evaporation. If gamma rays are absorbed through a single-particle mechanism we can assume that about half of the integrated gamma absorption cross section $\sigma_\gamma^{int} \approx \sigma_{\gamma p}^{int} + \sigma_{\gamma n}^{int}$ represents absorption by proton shells. The fraction of these absorptions resulting in direct proton emission is thus $\delta_{exp} \approx 0.8\,\sigma_{\gamma p}^{int}/(\sigma_\gamma^{int}/2) \approx 20\%$ when $\sigma_{\gamma n}^{int}$ (Cu^{65}) = 1110 Mev-mb.[17]

The Wilkinson model[23] was used to estimate the same quantity, following the procedure of Lokan.[25]

It was assumed that transitions from the $4f_{7/2}$ shell are most important and that they determine the position of the maximum $E_{\gamma p}^{max}$. From the spectrum of protons emitted as a result of gamma irradiation with energy close to $E_{\gamma p}^{max}$ (Fig. 6b) it follows that particles emitted from the $4f_{7/2}$ shell have an average energy of $6 - 7$ Mev. We have found $\delta \approx 10\%$, using $r_0 = 1.5 \times 10^{-13}$ cm and W, the imaginary part of the complex potential, given by $2W = 4$ Mev.[25] The agreement with experiment is satisfactory, considering the roughness of the estimate.

The authors are deeply indebted to N. A. Ponomareva and R. D. Rozhdestvenskaya for scanning of the plates and assistance with the treatment of the data.

[1] O. Hirzel and H. Wäffler, Helv. Phys. Acta 20, 373 (1947).

[2] B. C. Diven and G. M. Almy, Phys. Rev. 80, 407 (1950).

[3] P. R. Byerly and W. E. Stephens, Phys. Rev. 83, 54 (1951).

[4] E. D. Courant, Phys. Rev. 82, 703 (1951).

[5] Lejkin, Osokina, and Ratner, Nuovo cimento Suppl. 3, 105 (1956).

[6] R. M. Osokina and B. S. Ratner, JETP 32, 30 (1957), Soviet Phys. JETP 5, 1 (1957).

[7] M. E. Toms and W. E. Stephens, Phys. Rev. 95, 1209 (1954).

[8] W. V. Weisskopf, Phys. Rev. 52, 295 (1937).

[9] R. M. Osokina and B. S. Ratner, Physica 22, 1147A (1956).

[10] Akindinov, Amirov, Osokina, and Ratner, Report at All-Union Conference on Nuclear Reactions, 1957.

[11] B. Forkman, Arkiv Fysik 11, 265 (1956).

[12] Medicus, Grant, and Demers, Bull. Am. Phys. Soc. 3, 382 (1958).

[13] J. Rotblat, Nature 167, 550 (1950).

[14] L. Katz and A. G. W. Cameron, Can. J. Phys. 29, 518 (1951).

[15] V. F. Weisskopf, Statistical Theory of Nuclear Interactions, Russ. Transl., IIL, 1952.

[16] J. M. Blatt and V. F. Weisskopf, Theoretical Nuclear Physics, Wiley, N. Y., 1952.

[17] L. Katz and A. G. W. Cameron, Can. J. Phys. 29, 1209 (1951).

[18] J. W. Butler and C. R. Gossett, Phys. Rev. 108, 1473 (1957).

[19] T. Ericson, Nuclear Phys. 11, 481 (1959).

[20] P. F. Klinkenberg, Revs. Modern Phys. 24, 63 (1952).

[21] D. L. Allan, Nuclear Phys. 6, 464 (1958).

[22] D. L. Allan, Proc. Phys. Soc. (London) A70, 195 (1957).

[23] D. H. Wilkinson, Physica 22, 1039 (1956).

[24] J. Eichler and H. A. Weidenmuller, Z. Physik 152, 261 (1958).

[25] K. H. Lokan, Proc. Phys. Soc. (London) A73, 697 (1959).